

Electronic Supplementary Information (ESI)

Templating fabrication of hierarchically porous metal–organic frameworks and simulation of crystal growth

Chongxiong Duan,^a Hang Zhang,^a Minhui Yang,^a Feier Li,^a Yi Yu,^a Jing Xiao,^a Hongxia Xi*^{a, b}

^aSchool of Chemistry and Chemical Engineering, South China University of Technology, Guangzhou 510640, China.

^bGuangdong Provincial Key Laboratory of Atmospheric Environment and Pollution Control, South China University of Technology, Guangzhou Higher Education Mega Centre, Guangzhou 510006, PR China.

Experimental section

Chemicals. Copper nitrate trihydrate ($\text{Cu}(\text{NO}_3)_2 \cdot 3\text{H}_2\text{O}$), 1,3,5-benzenetricarboxylic acid (H_3BTC), zinc acetate dihydrate ($\text{Zn}(\text{CH}_3\text{CO}_2)_2 \cdot 2\text{H}_2\text{O}$), 2-methylimidazole (2Im), zinc oxide (ZnO), *N,N*-dimethyloctylamine (DMOA), *N,N*-dimethyldodecylamine (DMDA), and *N,N*-dimethylformamide (DMF), above chemicals were purchased from J&K or aladdin Chemical Ltd, and utilized without further purification.

Solvothermal synthesis of conventional Cu-BTC

The conventional microporous Cu-BTC was prepared according to the procedures reported,¹ and the obtained product is denoted as C-Cu-BTC.

Rapid room-temperature synthesis of hierarchically porous Cu-BTC with *N,N*-dimethyldodecylamine as template

The experimental procedures are similar to the synthesis of H-Cu-BTC, except the *N,N*-dimethyloctylamine (DMOA) was replaced by *N,N*-dimethyldodecylamine (DMDA). The resulting product is denoted as H-Cu-BTC_A.

Rapid synthesis of hierarchically porous ZIF-8 under facile conditions

The experimental procedures are similar to the previously reported methods,^{2, 3} firstly, 5 mmol of zinc oxide (ZnO) was added to 10 mL of deionized water as solution A, and 5 mmol of zinc acetate dihydrate ($\text{Zn}(\text{CH}_3\text{CO}_2)_2 \cdot 2\text{H}_2\text{O}$) was added to 5 mL of *N,N*-dimethylformamide (DMF) as solution B. After that, two solutions were mixed under fast magnetic stirring (denoted as solution C), and continue stirring for 16 h. The formation of gel-like viscous fluid indicates that the

formation of (Zn, Zn) hydroxy double salt (HDS).³ After that, 3 mmol of 2-methylimidazole (2Im) and 3 mmol of DMOA were added to 15 mL methanol (denoted as solution D), and stirring for 15 min. Then, 2 mL of (Zn, Zn) HDS suspension was added to solution D, and then continue stirring for 10 min. Subsequently, the precipitate was collected by filtered and immersed in ethanol four times at 60 °C for 48 h, and then dried overnight in an oven at 120 °C. The resulting product is denoted as H-ZIF-8. Similarly, hierarchically porous ZIF-8 synthesized with DMDA as template is denoted as H-ZIF-8_A.

Table S1 Flory-Huggins interaction parameter χ_{ij} between various beads used in this work.

Bead ^a	Y	W	B	Q	N	C
Y	0.00	0.196	0.514	4.08	0.156	3.53
W		0.00	2.74	4.50	-0.498	7.28
B			0.00	4.18	2.29	1.43
Q				0.00	4.23	13.9
N					0.00	3.08
C						0.00

Table S2 Textural properties of hierarchically porous Cu-BTC and conventional Cu-BTC.

Sample	S_{BET}^a [m ² ·g ⁻¹]	S_{micro}^b [m ² ·g ⁻¹]	S_{meso}^c	V_t^d [cm ³ ·g ⁻¹]	V_{meso}^e [cm ³ ·g ⁻¹]	V_{micro}^f [cm ³ ·g ⁻¹]
H-Cu-BTC	1110	926	184	0.61	0.17	0.43
H-Cu-BTC_1	1347	1153	194	0.66	0.12	0.54
H-Cu-BTC_5	765	640	125	0.44	0.14	0.30
H-Cu-BTC_A	563	453	110	0.59	0.38	0.21
H-ZIF-8	1660	1456	204	1.35	0.78	0.57
H-ZIF-8_1	1652	1469	183	1.24	0.70	0.54
H-ZIF-8_5	1617	1378	239	1.27	0.74	0.53
H-ZIF-8_A	1350	1098	252	1.19	0.68	0.51

^a S_{BET} : Brunauer–Emmett–Teller (BET) surface area; ^b S_{micro} : micropore surface area; ^c S_{meso} : mesopore surface area;

^d V_t : total pore volume; ^e V_{meso} : mesopore volume; ^f V_{micro} : micropore volume.

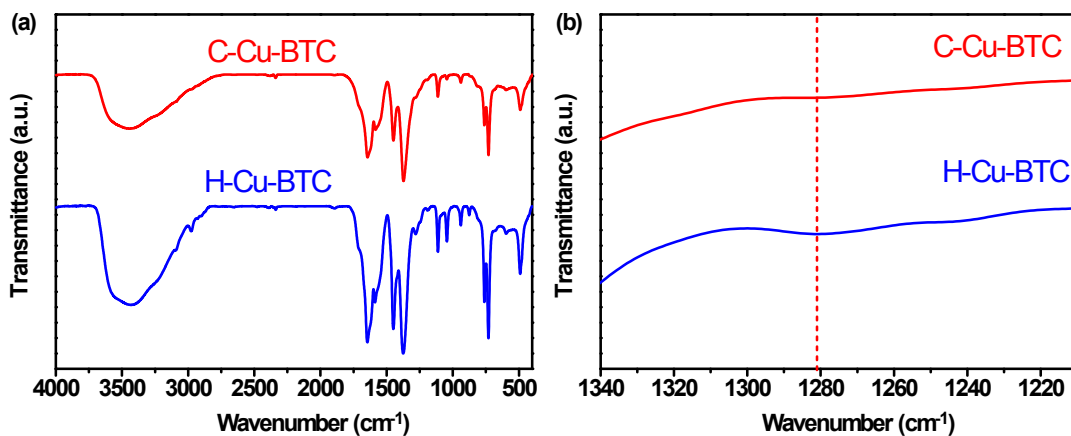


Fig. S1 (a) FTIR spectra of H-Cu-BTC and conventional Cu-BTC (C-Cu-BTC) samples, and (b) FTIR spectra of H-Cu-BTC sample in the narrow region of 1340–1210 cm⁻¹.

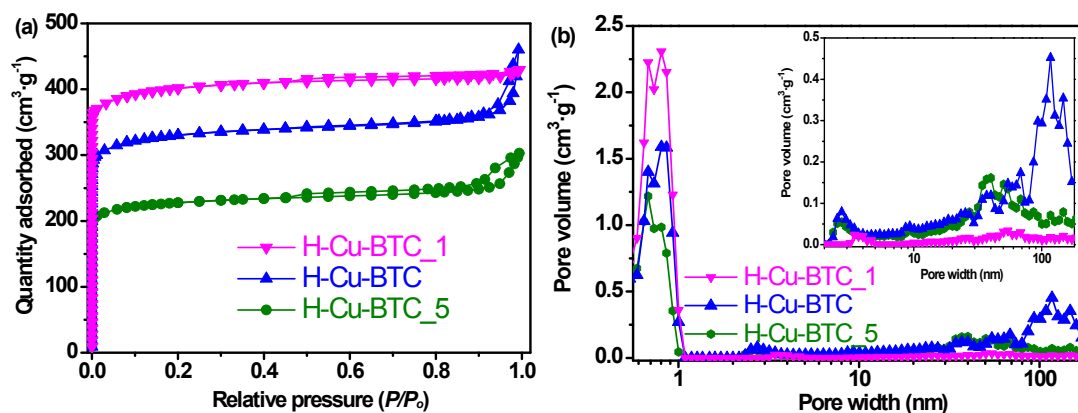


Fig. S2 (a) N₂ adsorption-desorption isotherms and (b) corresponding pore size distributions of H-Cu-BTC, H-Cu-BTC_1, and H-Cu-BTC_5 samples.

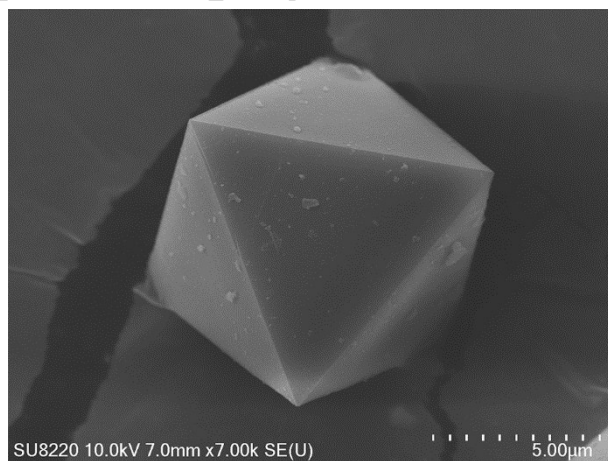


Fig. S3 SEM image of conventional Cu-BTC sample.

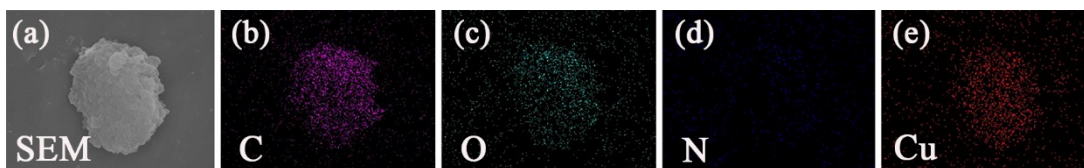


Fig. S4 Elemental distribution maps of H-Cu-BTC: (a) SEM, (b) C, (c) O, (d) N, and (e) Cu.

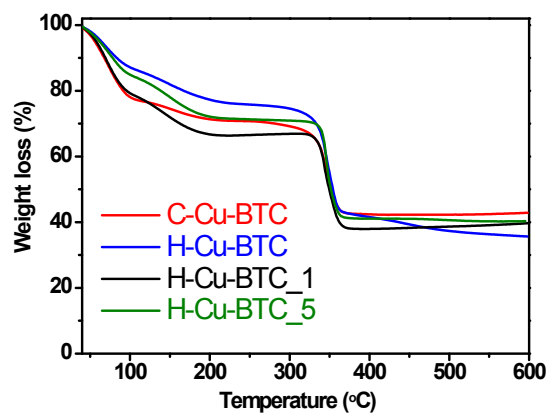


Fig. S5 Thermogravimetric analysis (TGA) of conventional Cu-BTC (C-Cu-BTC) and H-MOFs.

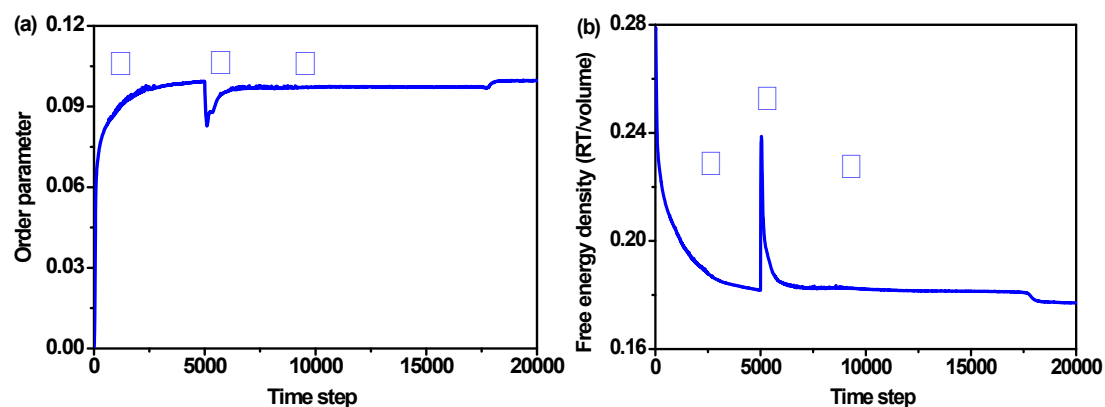


Fig. S6 (a) Time evolution of order parameter P , and (b) the free energy density plot with time step during the mesophase formation of hierarchically porous MOFs.

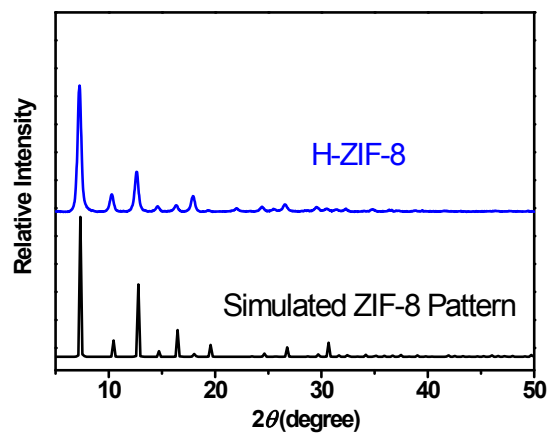


Fig. S7 Powder XRD patterns of H-ZIF-8 and the simulated ZIF-8 pattern.

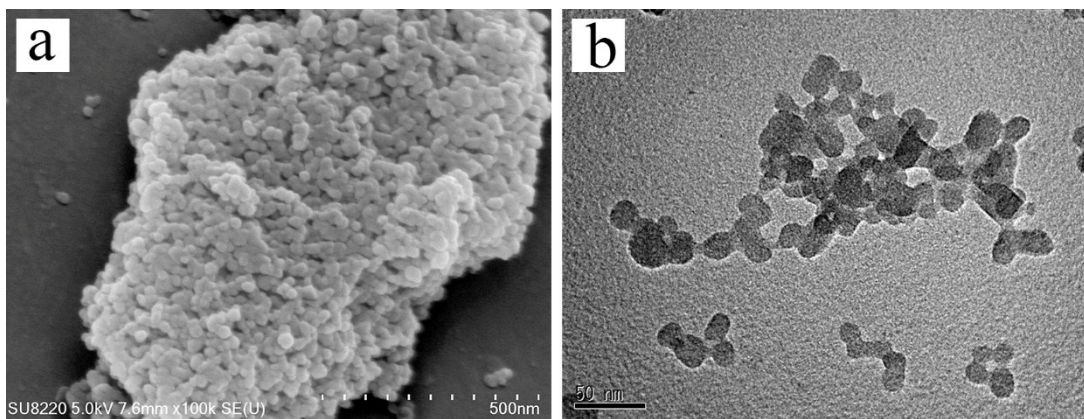


Fig. S8 (a) SEM and (b) TEM images of H-ZIF-8 sample.

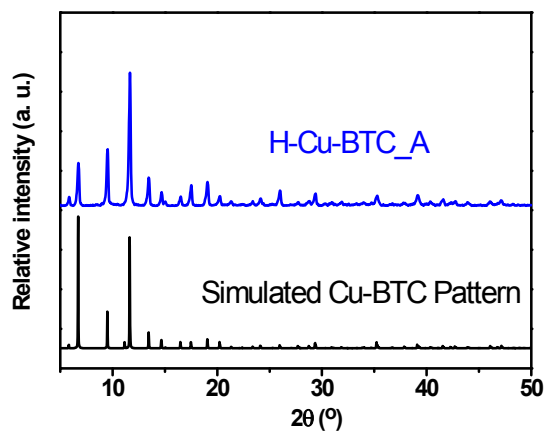


Fig. S9 Powder XRD patterns of H-Cu-BTC_A and the simulated Cu-BTC pattern.

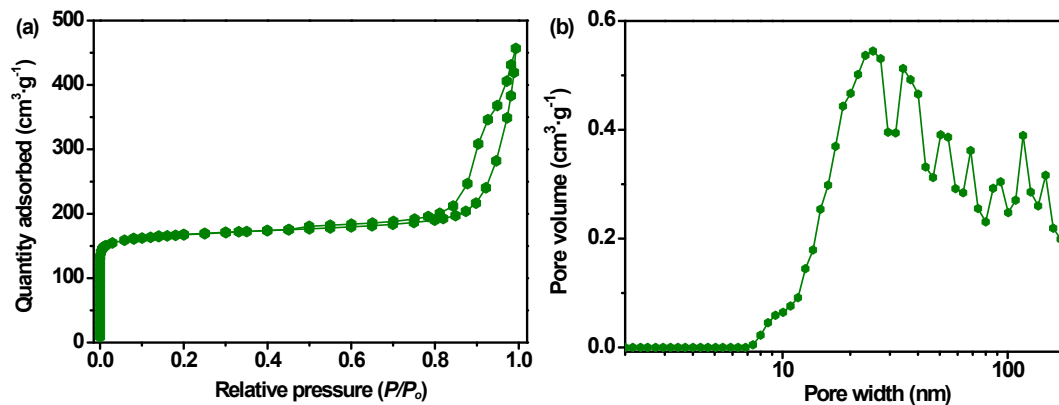


Fig. S10 (a) N₂ adsorption–desorption isotherms and (b) pore size distributions of H-Cu-BTC_A.

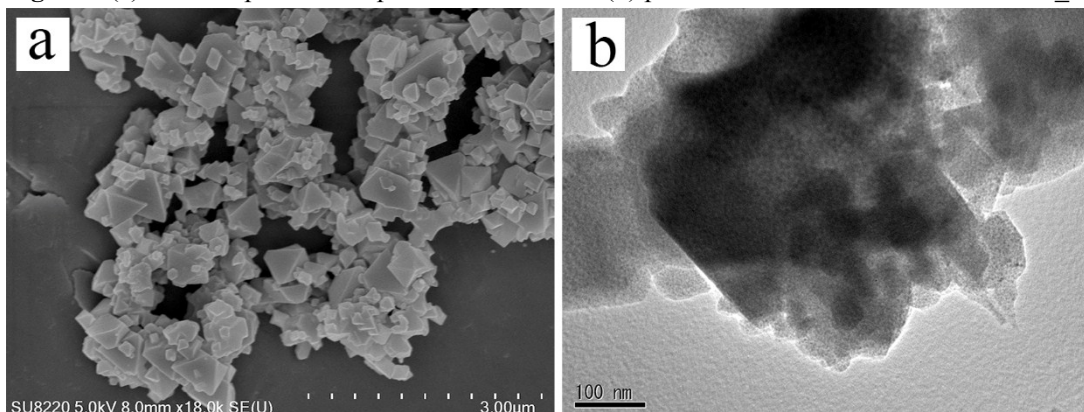


Fig. S11 (a) SEM and (b) TEM images of H-Cu-BTC_A sample.

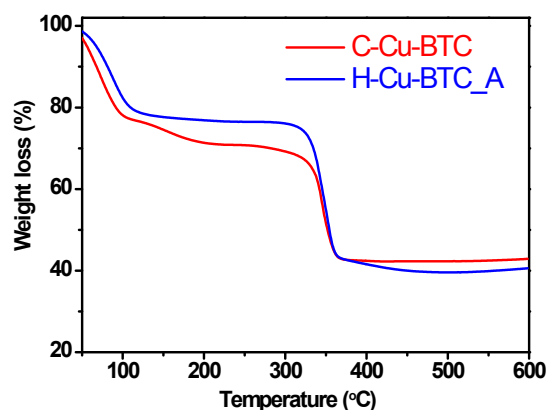


Fig. S12 TGA of H-Cu-BTC-A and C-Cu-BTC samples.

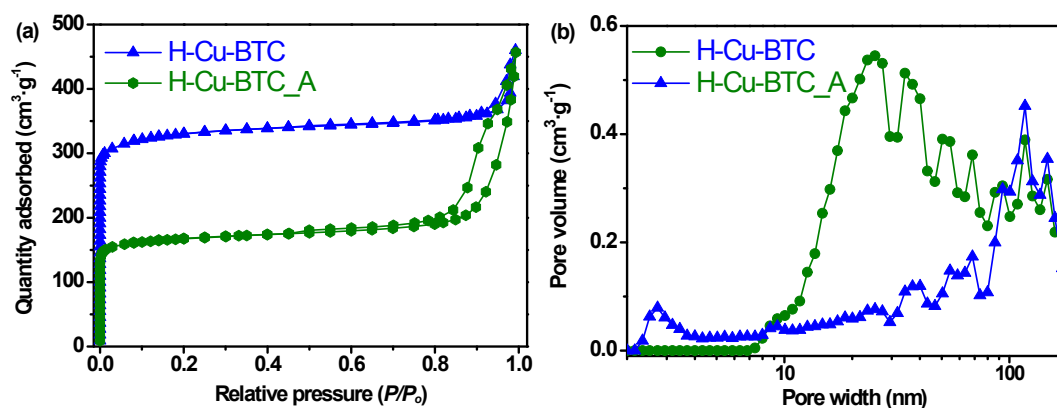


Fig. S13 (a) The N₂ adsorption–desorption isotherms and (b) the corresponding pore size distributions of H-Cu-BTC and H-Cu-BTC_A samples.

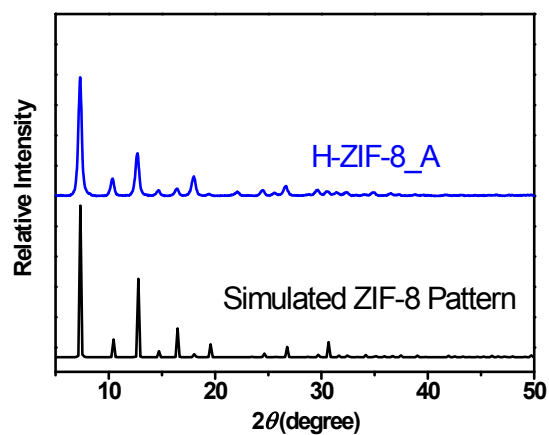


Fig. S14 Powder XRD patterns of H-ZIF-8_A and the simulated ZIF-8 pattern.

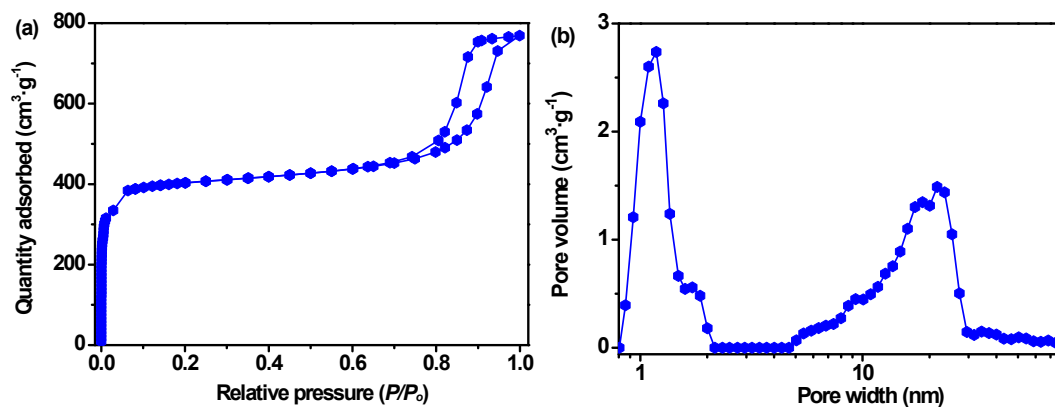


Fig. S15 (a) N_2 adsorption–desorption isotherms and (b) pore size distributions of H-ZIF-8_A.

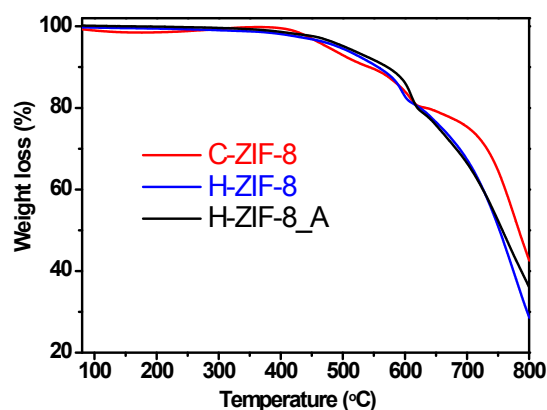


Fig. S16 TGA of H-ZIF-8, H-ZIF-8_A, and conventional ZIF-8 (C-ZIF-8) samples.

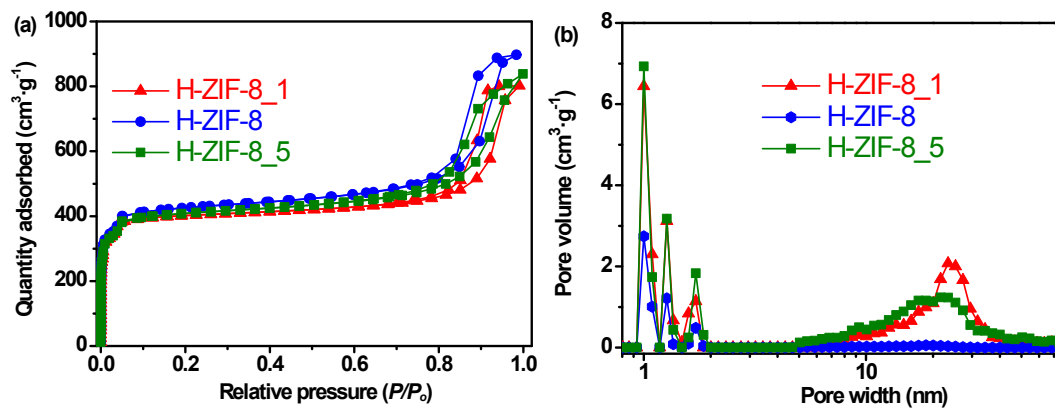


Fig. S17 (a) N_2 adsorption–desorption isotherms and (b) corresponding pore size distributions of H-ZIF-8_1, H-ZIF-8, and H-ZIF-8_5 samples.

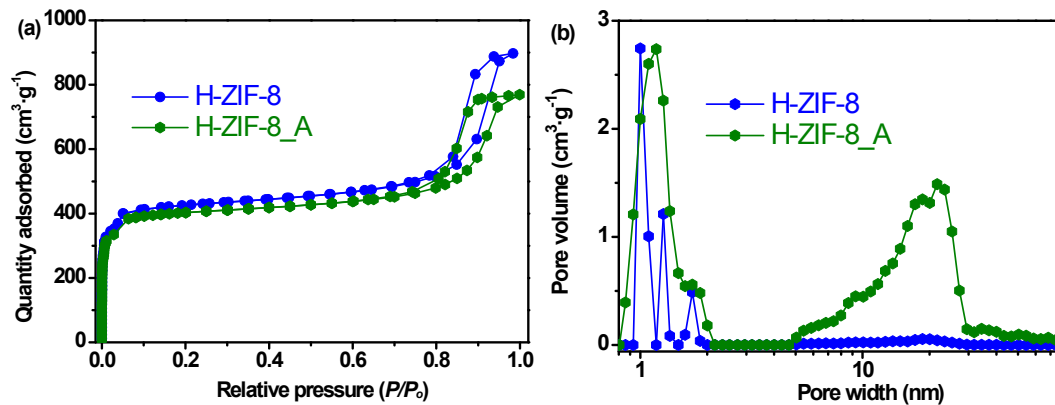


Fig. S18 (a) N_2 adsorption–desorption isotherms and (b) corresponding pore size distributions of H-ZIF-8 and H-ZIF-8_A samples.

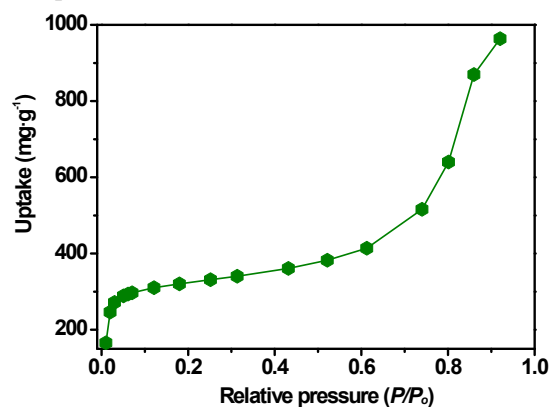


Fig. S19 Gaseous toluene sorption isotherms at 298K on H-ZIF-8 sample.

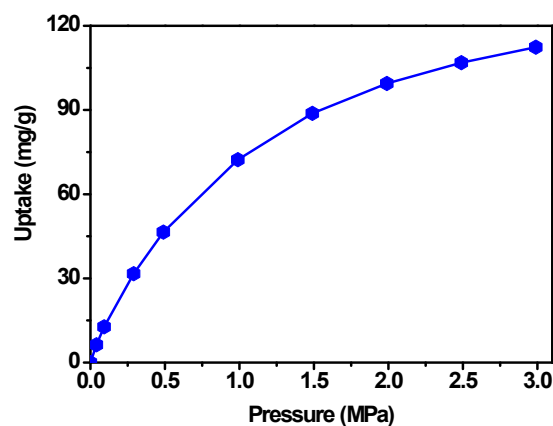


Fig. S20 CH_4 adsorption curve of H-Cu-BTC_A sample at 298 K.

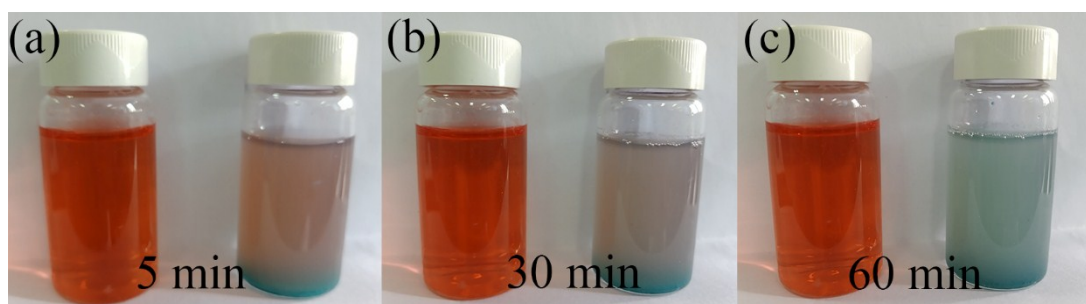


Fig. S21 Photograph of decoloration process for congo red (CR, $C_0 = 30 \text{ mg}\cdot\text{L}^{-1}$) solution with H-Cu-BTC_A ($m = 20 \text{ mg}$) adsorbent (right) at different times: (a) 5 min; (b) 30 min; and (c) 60 min.

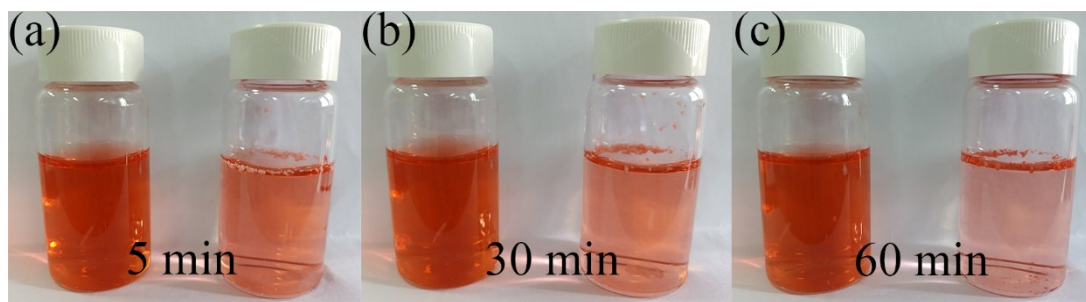


Fig. S22 Photograph of decoloration process for CR ($C_0 = 30 \text{ mg}\cdot\text{L}^{-1}$) solution with H-ZIF-8 ($m =$

20 mg) adsorbent (right) at different times: (a) 5 min; (b) 30 min; and (c) 60 min.

References

1. C. Duan, F. Li, H. Zhang, J. Li, X. Wang and H. Xi, *RSC Adv.*, 2017, 7, 52245-52251.
2. C. Duan, F. Li, L. Li, H. Zhang, X. Wang, J. Xiao and H. Xi, *CrystEngComm*, 2018, 20, 1057-1064.
3. J. Zhao, W. T. Nunn, P. C. Lemaire, Y. Lin, M. D. Dickey, C. J. Oldham, H. J. Walls, G. W. Peterson, M. D. Losego and G. N. Parsons, *J. Am. Chem. Soc.*, 2015, 137, 13756-13759.